JPET Fast Forward. Published on September 24, 2009 as DOI: 10.1124/jpet.109.159020

Title Page

Nicotinamide glycolates antagonize CXCR2 activity through an intracellular mechanism

Dean Y. Maeda, Mark T. Quinn, Igor A. Scheptekin, Liliya N. Kirpotina, and John A. Zebala

Syntrix Biosystems, Inc., Auburn, Washington (D.Y.M., J.A.Z.), Department of Veterinary Molecular Biology, Montana State University, Bozeman, Montana (M.T.Q., I.A.S., L.N.K.), Department of Laboratory Medicine, University of Washington, Seattle, Washington (J.A.Z.)

Running Title Page

Running title: Nicotinamide glycolates are intracellular CXCR2 antagonists

Corresponding Author:

Dean Y. Maeda, Ph.D.

Syntrix Biosystems, Inc.

215 Clay Street NW

Suite B-5

Auburn, WA 98001

phone: 253-833-8009

fax: 253-833-8127

e-mail: dmaeda@syntrixbio.com

Number of text pages: 35

Number of tables: 2

Number of figures: 9

Number of references: 36

Number of words in Abstract: 242

Number of words in Introduction: 574

Number of words in Discussion: 1416

Abbreviations:

AMD3100, 1,1′-[1,4-phenylenebis(methylene)]bis [1,4,8,11-tetraazacyclotetradecane] octohydrobromide dehydrate; ANOVA, analysis of variance; BX471, *N*-(5-chloro-2-(2-(4-((4-

JPET Fast Forward. Published on September 24, 2009 as DOI: 10.1124/jpet.109.159020
This article has not been copyedited and formatted. The final version may differ from this version.

fluorophenyl)methyl)-2-methyl-1-piperazinyl)-2-oxoethoxy) phenyl)urea hydrochloric acid; CCR1/2/3/9, chemokine (C-C motif) receptor 9; CHO, Chinese hamster ovary; CXCL1/2/3, growth-related oncogenes α, β and γ (GRO α/β/γ); CXCL5, epithelial-derived neutrophil-activating peptide 78 (ENA-78); CXCL6, granulocyte chemotactic protein-2; CXCL7 neutrophil-activating protein-2 (NAP-2); CXCL8, interleukin-8 (IL-8); DMF, dimethylformamide; DMSO, dimethylsulfoxide; EEDQ, 2-ethoxy-1-ethoxycarbonyl-1,2-dihydroquinoline; ELR, glutamine-leucine-arginine motif; EtOH, ethanol; Fura-2AM, acetoxymethyl 2-[5-[bis[(acetoxymethoxy-oxo-methyl)methyl]amino]-4-[2-[2-[bis[(acetoxymethoxy-oxo-methyl)methyl]amino]-5-methyl-phenoxy]ethoxy]benzofuran-2-yl]oxazole-5-carboxylate; [^{35}S]GTPγS, guanosine 5′-[γ-^{35}S]-triphosphate, triethylammonium salt; HBSS, Hank's balanced salt solution; HBSS^{-}, HBSS without Ca^{2+} and Mg^{2+}; HPLC, high-pressure liquid chromatography; LC-MS/MS, liquid-chromatography – mass spectrometry/mass spectrometry (tandem mass spectrometry); MeCN, acetonitrile; MRM, multiple reaction monitoring mode; OAT, organic anion transporter; PBS, phosphate buffered saline; PMN, polymorphonuclear leukocyte; Repertaxin, [(*R*)(-)-2-(4-isobutylphenyl)propionyl methanesulfonamide], RPMI, Roswell Park Memorial Institute, SB265610, [1-(2-bromo-phenyl)-3-(7-cyano-3H-benzotriazol-4-yl)-urea]; SCH527123, [2-hydroxy-N,N,-dimethyl-3-[[2-[[1(*R*)-(5-methyl-2-furanyl)propyl]amino]-3,4-dioxo-1-cyclobuten-1-yl]amino]benzamide]; TAK-799, (*N*,*N*-dimethyl-*N*-[4-[[[2-(4-methylphenyl)-6,7-dihydro-5*H*-benzocyclohepten-8-yl]carbon- yl]amino]benzyl]-tetrahydro-2*H*-pyran4-aminium chloride; THF, tetrahydrofuran.

Recommended Section Assignment:

Cellular and Molecular

Abstract

The chemokine receptors CXCR1/2 are involved in a variety of inflammatory diseases, including chronic obstructive pulmonary disease (COPD). Several classes of allosteric small-molecule CXCR1/2 antagonists have been developed. The data presented herein describe the cellular pharmacology of the acid and ester forms of the nicotinamide glycolate pharmacophore, a potent antagonist of CXCR2 signaling by the chemokines CXCL1 and CXCL8. Ester forms of the nicotinamide glycolate antagonized CXCL1-stimulated chemotaxis (IC_{50} = 42 nM) and calcium flux (IC_{50} = 48 nM) in human neutrophils, but were inactive in cell-free assays of [^{125}I]-CXCL8/CXCR2 binding and CXCL1-stimulated [^{35}S]GTPγS exchange. Acid forms of the nicotinamide glycolate were inactive in whole-cell assays of chemotaxis and calcium flux, but inhibited [^{125}I]-CXCL8/CXCR2 binding and CXCL1-stimulated [^{35}S]GTPγS exchange. The [^{3}H]-ester was internalized by neutrophils and rapidly converted to the [^{3}H]-acid in a concentrative process. The [^{3}H]-acid was not internalized by neutrophils, but was sufficient alone to inhibit CXCL1-stimulated calcium flux in neutrophils that were permeabilized by electroporation to permit its direct access to the cell interior. Neutrophil efflux of the acid was probenecid-sensitive, consistent with an organic acid transporter. These data support a mechanism wherein the nicotinamide glycolate ester serves as a lipophilic precursor that efficiently translocates into the intracellular neutrophil space to liberate the active acid form of the pharmacophore, which then acts at an intracellular site. Rapid inactivation by plasma esterases precluded usage *in vivo*, but the mechanism elucidated provided insight for new nicotinamide pharmacophore classes with therapeutic potential.

Introduction

Chemoattractant cytokines, or chemokines, promote the directed migration of polymorphonuclear leukocytes (PMNs) to sites of inflammation in a process known as chemotaxis. Among the most important chemokines released during inflammatory responses are the "Cys-Xaa-Cys" (CXC) or α chemokines, which are characterized by the presence of an intervening amino acid between conserved cysteines. Specifically, the Glu-Leu-Arg (ELR) motif-containing CXC chemokines are major PMN chemoattractants and activate these cells via two G protein-coupled CXC receptors (CXCRs) known as CXCR1 and CXCR2 (Holmes et al., 1991; Murphy and Tiffany, 1991; Cerretti et al., 1993; Geiser et al., 1993). CXCR1 preferentially binds interleukin-8 (IL-8, CXCL8), but can also bind granulocyte chemotactic protein-2 (GCP-2, CXCL6) with lower affinity. By comparison, CXCR2 binds growth-related oncogenes α, β and γ (GRO α/β/γ, CXCL1/2/3), epithelial-derived neutrophil-activating peptide 78 (ENA-78, CXCL5), neutrophil-activating protein-2 (NAP-2, CXCL7), CXCL6 and CXCL8.

CXCR1, CXCR2, and their chemokine ligands are involved in a wide range of acute and chronic inflammatory diseases, including acute respiratory distress syndrome (Kurdowska et al., 2002), rheumatoid arthritis (Erdem et al., 2005; Lally et al., 2005), psoriasis (Reich et al., 2001), inflammatory bowel disease (Banks et al., 2003), chronic obstructive pulmonary disease (COPD) and asthma (Keatings et al., 1996; Beeh et al., 2003; Chapman et al., 2009), cystic fibrosis (Koller et al., 1997) and atherosclerosis (Bizzarri et al., 2006). CXCR1 and CXCR2 have thus garnered much attention as targets for small-molecule drug discovery and have prompted the development of several potent small molecule antagonists, several of which have progressed into clinical trials. These include the CXCR1-selective antagonist repertaxin [(*R*)(-)-2-(4-isobutylphenyl)propionyl methanesulfonamide] (Bertini et al., 2004; Allegretti et al., 2005) and a

series of CXCR2-selective diarylureas, as exemplified by SB265610 [1-(2-bromo-phenyl)-3-(7-cyano-3H-benzotriazol-4-yl)-urea] (White et al., 1998; Auten et al., 2001; Podolin et al., 2002). Derivatives of the latter series, wherein the urea was replaced with the 3,4-diaminocyclobut-3-ene-1,2-dione bioisostere, led to antagonists with picomolar affinity for CXCR2, such as SCH527123 [2-hydroxy-N,N,-dimethyl-3-[[2-[[1(R)-(5-methyl-2-furanyl)propyl]amino]-3,4-dioxo-1-cyclobuten-1-yl]amino]benzamide] (Dwyer et al., 2006; Merritt et al., 2006). Consistent with the relatively large binding surface between CXCR1/2 and their chemokine ligands, studies have found that repertaxin, SB265610, SCH527123, and related analogues all act as allosteric inhibitors (Bertini et al., 2004; Casilli et al., 2005; Garau et al., 2006; Gonsiorek et al., 2007; Moriconi et al., 2007; Nicholls et al., 2008; Bradley et al., 2009; de Kruijf et al., 2009).

Our CXCR1/2 antagonist discovery efforts have focused on refinement and pharmacological characterization of the nicotinamide glycolate pharmacophore (Fig. 1). While a representative nicotinamide glycolate methyl ester **1** of this class was shown to potently antagonize CXCL1-mediated chemotaxis of primary human PMNs *in vitro* with an IC_{50} of 42 nM (Cutshall et al., 2002), pharmacological mechanisms were not evaluated. Through the use of tritiated derivatives and direct electroporation of compounds into PMNs, we show that the methyl ester form (e.g., **3**) permeates through the PMN cell membrane, is rapidly hydrolyzed to the nicotinamide glycolate acid (e.g., **4**), and then accumulates intracellularly to millimolar concentrations, where it acts as a CXCR2 antagonist. The accumulated acid is subject to efflux from the cell by a probenecid-sensitive transporter, most likely an organic anion transporter (OAT). The studies presented herein thus describe the pharmacology of certain hydrolytically-sensitive forms of this pharmacophore class, and demonstrate that the nicotinamide glycolates require intracellular access to antagonize CXCR2 signaling. The implications of these findings

are discussed with regard to developing future related structural classes of compounds based on this pharmacophore, which may be suitable for therapeutic implementation.

JPET Fast Forward. Published on September 24, 2009 as DOI: 10.1124/jpet.109.159020
This article has not been copyedited and formatted. The final version may differ from this version.

Methods

Chemistry. All chemicals and reagents for synthesis were purchased from Sigma-Aldrich (Milwaukee, WI), and solvents were purchased from VWR International (West Chester, PA). All reagents and solvents were used as received. Compounds **1** – **6** are: **1**, [5-(4-fluoro-phenylcarbamoyl)-pyridin-2-ylsulfanyl]-acetic acid methyl ester; **2**, [5-(4-fluoro-phenylcarbamoyl)-pyridin-2-ylsulfanyl]-acetic acid; **3**, [5-(4-fluoro-phenylcarbamoyl)-pyridin-2-yloxy]-acetic acid methyl ester; **4**, [5-(4-fluoro-phenylcarbamoyl)-pyridin-2-yloxy]-acetic acid; **5**, [5-(4-fluoro-phenylcarbamoyl)-pyridin-2-ylsulfanyl]-acetic acid benzyl ester; and **6**, [5-(4-fluoro-phenylcarbamoyl)-pyridin-2-ylsulfanyl] acetic acid *tert*-butyl ester. Compounds **1** – **4** were prepared as described by Cutshall *et al*. (Cutshall et al., 2002), and synthetic methods and characterization of compounds **5** and **6** are detailed in the Data Supplement (Supplemental Data). To prepare the tritiated derivatives of **3** and **4** (Fig. 2), 5,6-dicloro-nicotinic acid was coupled with 4-fluoroaniline using 2-ethoxy-1-ethoxycarbonyl-1,2-dihydroquinoline (EEDQ) to yield **7** (5,6-dichloro-*N*-(4-fluoro-phenyl)-nicotinamide) in 72% yield. Compound **7** was then treated with methyl glycolate and sodium hydride to form the glycolate methyl ester **8** ([3-chloro-5-(4-fluoro-phenylcarbamoyl)-pyridin-2-ylsulfanyl]-acetic acid methyl ester) in 55% yield. The methyl ester was saponified to yield the corresponding acid **9** ([3-chloro-5-(4-fluoro-phenylcarbamoyl)-pyridin-2-ylsulfanyl]-acetic acid) in quantitative yield through the use of aq. LiOH in MeOH. The chloro-substituted ester and acid were then treated with tritium gas over a heterogeneous catalyst (Moravek Biochemicals, Brea, CA). Synthetic methods and characterization data for compounds [^{3}H]-**3**, [^{3}H]-**4**, and **7** – **9** are detailed in the Data Supplement (Supplemental Data).

Isolation of Human Neutrophils. Blood was collected from healthy donors in accordance with a protocol approved by the Institutional Review Board at Montana State University and the Declaration of Helsinki. PMNs were purified from human blood using dextran sedimentation, followed by Histopaque 1077 gradient separation and hypotonic lysis of red blood cells, as described previously (Siemsen et al., 2007). PMN preparations were routinely >95% pure, as determined by light microscopy, and >98% viable, as determined by trypan blue exclusion.

Uptake and Efflux Assays. Cell uptake was measured by incubating PMNs ($6x10^7$ cells) in 8 ml of Hank's balanced salt solution (HBSS) with 0.55, 0.20, 1.0 and 10.0 μM of [^{3}H]-**4** or [^{3}H]-**3**. Aliquots were taken from each concentration at 5, 20, 60 and 90 minutes, washed with HBSS, and centrifuged to pellet the cells. The molar amount of radioactivity internalized in the cell pellet was quantitated by scintillation (LS-6500 Liquid Scintillation Counter, Beckman Coulter, Fullerton, CA) and correlated with a calibration curve for each tritiated derivative. Efflux studies were performed by loading PMNs ($6x10^7$ cells in 8 ml HBSS) with the carboxylic acid [^{3}H]-**4** by a 20 min incubation with 20 μCi of the methyl ester [^{3}H]-**3**, followed by washing and then resuspending the cells in 20 ml HBSS. Aliquots from this cell suspension were then taken at 5, 15, 30, 60 and 90 minutes and centrifugated. The supernatant was analyzed by reverse-phase HPLC using a Shimadzu Class Vp system with a Phenomenex Jupiter C_{18} column (5 μm, 300 Å, 25 cm x 0.46 cm) and eluted with acetonitrile/water (60%/40%, v/v) containing 0.1% (v/v) TFA at a flow rate of 1 ml/min. The amount of [^{3}H]-**4** and [^{3}H]-**3** was quantitated by scintillation and integrating peak radioactivity (see method for detecting conversion of [^{3}H]-**3** to [^{3}H]-**4** below). For studies that examined the effect of probenecid on efflux, cells were loaded as described above, except that cells were resuspended in 25 ml HBSS with and without 2 mM

probenecid [*p*-(dipropylsulfamoyl)benzoic acid]. Probenecid HCl is acidic, and was buffered with NaOH and then diluted in HBSS before use to exclude any effect due to pH on efflux.

Intracellular Conversion of [^{3}H]-3 to [^{3}H]-4. PMNs ($6x10^7$ cells in 8 ml of HBSS) were incubated with 5 μCi of [^{3}H]-**3**, washed, then lysed with 100 μL 0.1% Triton X-100 at 0, 5 and 20 minutes and the lysate subjected to reverse-phase HPLC and scintillation counting, as described above. Radioactivity in peaks with retention times corresponding to **3** and **4** was integrated to determine the relative amounts of intracellular [^{3}H]-**3** and [^{3}H]-**4**, respectively.

Calcium Flux Assay. PMNs (3.1×10^7 cells in 1.7 ml) were suspended in HBSS without Ca^{2+} and Mg^{2+} ($HBSS^-$) containing 10 mM HEPES and Fura-2AM dye (2 μg/ml final concentration). Cells were aliquoted and treated with the indicated compounds or control DMSO (1% DMSO final concentration for both compound and control) for 30 min at 37°C. After dye loading, the samples were centrifuged at 3,000 x g for 1 min, the supernatants were removed, and the cell pellets were resuspended in HBSS containing 10 mM HEPES. The test compounds or DMSO (control) were added again at the same concentrations that were used during cell loading, and the cells were aliquoted into a 96-well microtiter plate (10^5 cells/well). After 15 sec of reading the basal level of fluorescence, CXCL1 or $HBSS^-$ were added (final concentration of CXCL1 was 25 nM, and changes in fluorescence were monitored (λ_{ex} = 340 nm, λ_{em} = 380 nm) every 5 s for 240 to 500 s at room temperature using a Fluoroscan Ascent FL microplate reader (ThermoElectron, Milford, MA). Maximum change in the ratio of fluorescence values at excitation wavelengths of 340 and 380 nm, expressed in arbitrary units over baseline (Max-Min), was used to determine the response. The effect of each compound on the CXCL1 response was normalized and expressed as a percent of the DMSO control, which was designated as "100% response." Curve fitting and calculation of the compound inhibitory concentration that reduced

the level of the CXCL1 response by 50% (IC_{50}), or the compound agonist concentration that increases the level of the calcium release by 50% of the maximum agonist-induced change (EC_{50}) were determined by nonlinear regression analysis of the dose-response curves generated using Prism 4 (GraphPad Software, Inc., San Diego, CA).

Human Neutrophil Electroporation. PMNs were electroporated on ice using 2 discharges of a 25 μFd capacitor at 1.75-2.5 kV/cm with a BioRad Gene Pulser II (BioRad, Richmond, CA) as described previously (DeLeo et al., 1996). Analysis of aliquots of the cells for trypan blue exclusion indicated 96-98% of the cells were permeabilized. Permeabilized cells were transferred to 6-well tissue culture plates containing RPMI/10% FBS without (no compound control) and with the indicated concentrations of test compound **2** (no DMSO was added for test compound or control, since the acid **2** was soluble in aqueous solution without requiring DMSO). After a 30 min incubation at 37^{o}C and 5% CO_2, the cells were collected, washed, and resuspended in HBSS containing 0.1% bovine serum albumin. Analysis of aliquots of the cells for trypan blue exclusion indicated 97-98% of the cells recovered and excluded trypan blue.

De-Esterification in Human Plasma. A 1 mM stock solution of the test compound was prepared in DMSO and serially diluted to a concentration of 10 μM in PBS. A 100 μl aliquot of the 10 μM test solution was added to 900 μl of previously frozen pooled human plasma (Innovative Research, Novi, MI) to yield a 1 μM final concentration with 0.1% DMSO. The plasma solutions were then incubated at 37^{o}C, and 100 μl aliquots were removed at time points 0, 15, 30, 60, 120, and 240 min, and diluted with 300 μl MeCN containing 1 μM internal standard. The precipitated proteins were centrifuged, and the supernatant was decanted and analyzed by LC-MS/MS using a Micromass Quattro II mass spectrometer (Waters, Milford, MA) connected

to a Shimadzu 10AD HPLC system (Shimadzu, Kyoto, Japan) employing separation conditions identical to those used for evaluation of product purity (Supplemental Data). Multiple reaction monitoring (MRM) mode was used for detection of esters **1**, **5**, **6** and the internal standard. The first quadrupole (Q1) was set to transmit the precursor ions MH+ at m/z 320.9 for **1**, 396.9 for **5**, 363.1 for **6**, and 473.9 for the internal standard. The product ions were monitored in the third quadrupole (Q3) at m/z 109.8 for both esters **1** and **6**, 90.8 for **5**, and at 134.9 for the internal standard. The product ion peaks were integrated, and normalized to the internal standard product ion peak.

Results

Pharmacologic Parameters of Nicotinamide Glycolates 1 – 4. Pharmacologic parameters in the CXCR2 signaling pathway were defined for compounds **1** – **4** (Table 1). The nicotinamide glycolate methyl ester **1** was a potent antagonist in whole-cell assays of CXCL-mediated chemotaxis (IC_{50} = 42 nM) and calcium flux (IC_{50} = 48 nM) in PMNs, but surprisingly exhibited no antagonism in cell-free CXCR2 assays of either [^{125}I]-CXCL8 binding, [^{125}I]-CXCL1 binding, or CXCL1-stimulated [^{35}S]GTPγS exchange (Table 1). Conversely, the corresponding nicotinamide glycolate carboxylic acid **2** lacked activity in whole-cell assays of chemotaxis and calcium flux in PMNs, but inhibited both radiolabeled CXCL8 binding (IC_{50} = 1.2 μM) and CXCL1-stimulated [^{35}S]GTPγS exchange (IC_{50} = 0.61 μM) in CXCR2 membranes. The equipotent but oxygen-containing nicotinamide glycolates **3** and **4** exhibited a similar activity profile in cell-free assays of [^{125}I]-CXCL8 and [^{125}I]-CXCL1 binding to CXCR2 membranes, and in whole-cell assays of CXCL1-mediated chemotaxis and calcium flux. Absent antagonism at N-formyl peptide receptors, CCR1, CCR2, CCR3 and CCR9 supported the CXCR2-selectivity of compounds **1** – **4** (Cutshall et al., 2002). The structure-activity-relationship (SAR) of **1** and **2** in cell-free assays indicated that methyl esterification of the carboxylic acid was a sufficient perturbation to render **2** inactive at CXCR2. The correlation between negative charge and absent activity of the nicotinamide glycolates in whole-cell assays suggested that the cell membrane acted as a barrier to the passive diffusion of the carboxylic acid **2**, which was otherwise active in cell-free assays. Based on these observations, we postulated that the uncharged and inactive methyl ester **3** accesses the intracellular space by passive diffusion, where it is de-esterified to form the active carboxylic acid **2** that then binds an intracellular site and antagonizes CXCR2.

JPET Fast Forward. Published on September 24, 2009 as DOI: 10.1124/jpet.109.159020
This article has not been copyedited and formatted. The final version may differ from this version.

Uptake of Methyl Ester [^{3}H]-3 and Carboxylic Acid [^{3}H]-4. In order to quantify potential differences in the rate and magnitude of nicotinamide glycolate uptake between the acid and ester forms, PMNs were incubated over 90 minutes with varying concentrations of ester [^{3}H]-**3** or acid [^{3}H]-**4**. Aliquots were removed at various times, and the amount of tritiated compound internalized was quantified by scintillation (Fig. 3). In the case of ester [^{3}H]-**3**, the amount of radioactivity internalized dramatically increased as a function of extracellular concentration and time, reaching intracellular concentrations 100- to 1000-fold greater than the extracellular concentration. At the highest extracellular concentration tested, incubation of PMNs in 10 μM [^{3}H]-**3** for 90 minutes resulted in the internalized radioactivity reaching an intracellular concentration of ~3 mM based on a mean PMN volume of 334 femtoliter (Nibbering et al., 1990). In contrast, the uptake of acid [^{3}H]-**4** was very limited, with intracellular accumulation detected only at the highest concentration tested. These data confirmed that the methyl ester was readily internalized into the PMN intracellular space, but the corresponding acid was substantially excluded by the cellular membrane, which is consistent with intracellular access being vital to activity.

Intracellular De-Esterification of Methyl Ester [^{3}H]-3 to Carboxylic Acid [^{3}H]-4. The absence of antagonism of the methyl ester **1** in cell-free assays, together with vigorous cellular uptake and potent nanomolar antagonism of the esters in whole PMNs, led us to hypothesize that ester antagonism of CXCR2 signaling required conversion of the methyl ester to the corresponding acid within the PMN. To test this hypothesis, PMNs were incubated with [^{3}H]-**3** and the PMNs were then collected at various times over 60 minutes and lysed, and the lysates were analyzed to quantify the relative amounts of the methyl ester [^{3}H]-**3** and the corresponding acid [^{3}H]-**4** (Fig. 4). After 5 min incubation, virtually all radioactivity (>96%)

detected in the PMN lysate corresponded to the hydrolyzed acid form. There was no de-esterification of the methyl ester [^{3}H]-**3** in control experiments that subjected [^{3}H]-**3** to the same incubation and lysis conditions in the absence of cells (data not shown). These data indicate that the nicotinamide glycolate esters are rapidly converted intracellularly to the corresponding acid, and in combination with their absent activity in cell-free assays, suggest that the acid is the active intracellular antagonist.

Antagonism and Susceptibility to De-Esterification. The esterase susceptibilities of the nicotinamide glycolates were determined by incubation in previously frozen human plasma. Whereas the nicotinamide glycolate methyl ester **1** and benzyl ester **5** were rapidly de-esterified to the corresponding acid **2**, the sterically hindered *tert*-butyl ester **6** exhibited complete resistance to ester hydrolysis out to 240 min (Fig. 5). Susceptibility to de-esterification was found to correlate with activity of the ester precursor in antagonizing CXCL1-stimulated calcium flux in whole PMNs (Table 2), consistent with the liberated acid **2** being the active antagonist in the intracellular compartment. The 240-fold greater potency of benzyl ester **5** compared to methyl ester **1** was likely the result of its greater lipophilicity, as suggested by the calculated octanol:water partition coefficients (Table 2).

Electroporation of Carboxylic Acid 2 into PMNs. To directly evaluate the possibility that carboxylic acid **2** is the active antagonist that acts intracellularly, **2** was provided access to the intracellular compartment of PMNs through electroporation (Fig. 6). Whereas compound **2** in the absence of electroporation was unable to inhibit CXCL1-mediated calcium release in PMNs at an extracellular concentration up to 5 μM, electroporation of **2** enabled potent and significant inhibition of CXCL1-mediated intracellular calcium release at extracellular concentrations of 0.1, 0.5 and 1.0 μM (IC_{50} = 260 $\pm$ 30 nM, $^{**}p < 0.01$ relative to the untreated

control, one-way ANOVA, Dunnett's multiple comparison test). This was not an artifact of electroporation, since parallel controls lacking antagonist retained chemotactic and intracellular calcium release responses upon treatment with CXCL1. Trypan blue exclusion controls confirmed that PMN membranes had completely resealed at the time antagonism was measured. These data show that intracellular nicotinamide glycolate acid **2** alone is sufficient to affect potent CXCR2 antagonism in PMNs. This observation together with its rapid and nearly quantitative liberation from the methyl ester **1** strongly implicates the ester as an inactive precursor that gives rise to the corresponding acid **2** as the active intracellular antagonist.

Efflux of Carboxylic Acid [^{3}H]-4 from PMNs. The absence of antagonism of the carboxylic acid form of the nicotinamide glycolates in whole-PMN assays suggested that the cell membrane may be acting as a bidirectional barrier to diffusion that could potentially trap the active carboxylic acid liberated from the ester precursor inside the cell. To examine the ability of PMNs to efflux the carboxylic acid form of the nicotinamide glycolate, PMNs were loaded with the carboxylic acid [^{3}H]-**4** by incubation with the methyl ester [^{3}H]-**3** precursor (Fig. 7). At 30, 60 and 90 minutes, there was a significant accumulation of radioactivity in the supernatant compared to the amount in the supernatant at 5 minutes (**$p < 0.01$, one-way ANOVA, Dunnett's multiple comparison test). All the radioactivity was accounted for by the carboxylic acid [^{3}H]-**4**, with no methyl ester [^{3}H]-**3** precursor detected. These observations suggest that the cell membrane did not irreversibly trap the active carboxylic acid within the cell. Instead, the data are consistent with efflux of the nicotinamide glycolate carboxylic acid from the PMN.

The anionic nature of carboxylic acid [^{3}H]-**4** suggested that the observed efflux might be mediated by an organic anion transporter (OAT). To explore this possibility, we examined the effect of the OAT inhibitor probenecid on efflux of [^{3}H]-**4** from PMNs. PMNs were loaded with

the carboxylic acid [^{3}H]-**4** and exposed to probenecid (Fig. 8). Compared to untreated controls, probenecid significantly inhibited [^{3}H]-**4** efflux from PMNs, as measured by its accumulation in the supernatant (***$p < 0.001$, two-way ANOVA). Probenecid also significantly inhibited efflux, as measured by [^{3}H]-**4** loss from the cell pellet, and after 90 minutes there was ~2.5-fold more radioactivity in the probenecid-treated PMN pellets than in the untreated control pellets. These data suggest that a PMN OAT is responsible at least in part for efflux of the active nicotinamide glycolate carboxylic acid from the intracellular PMN compartment.

Kinetics of CXCR2 Inhibition in PMNs after Methyl Ester 1 Washout. The observed efflux of the active nicotinamide glycolate acid from PMNs led us to consider how efflux would impact the kinetics of CXCR2 inhibition after washout of the methyl ester **1** from the extracellular space (Fig. 9). To examine this further, PMNs were incubated in the presence or absence of 1 μM of methyl ester **1** for 30 min, loaded with the cell-permeable calcium dye Fura-2 and then thoroughly washed and resuspended in assay buffer. The intracellular CXCL1-stimulated calcium flux was measured at times ranging from 0 – 3.5 hours. To control for changes to intracellular calcium related to PMN viability over the course of the experiment, percent calcium flux is expressed relative to the dynamic range established by a positive and negative control at each time point. Compared to untreated PMNs, calcium flux was inhibited in PMNs treated with **1**, and this inhibition was sustained throughout the duration of the experiment (3.5 hours).

Discussion

CXCR2 has attracted considerable attention as a potential drug target because of its involvement in different inflammatory diseases, particularly chronic pulmonary inflammatory diseases such as COPD, where increased numbers of neutrophils in the sputum of patients has been shown to correlate with increased levels of IL-8 (Keatings et al., 1996; Chapman et al., 2009). As a consequence, different classes of small-molecule CXCR2 antagonists have been developed that appear to share a common mechanism of allosteric, rather than competitive inhibition (Bertini et al., 2004; Casilli et al., 2005; Garau et al., 2006; Gonsiorek et al., 2007; Moriconi et al., 2007; Nicholls et al., 2008; Bradley et al., 2009; de Kruijf et al., 2009). Allosteric inhibition is likely to be a common mechanism for drug leads arising from small-molecule screening efforts against chemokine receptors, given the large extracellular ligand-receptor interface that a competitive inhibitor must confront. Allosteric inhibition has thus been observed for small-molecules targeting other chemokine receptors, such as AMD3100 at CXCR4, TAK-779 at CCR5, and BX 471 at CCR1 (Allen et al., 2007).

In the case of CXCR1/2, studies have found that the antagonists repertaxin, SB265610, SCH527123, and their related analogues act as allosteric inhibitors. Whereas natural ligands like CXCL1/8 bind to the extracellular orthosteric binding site at the N-terminus and extracellular loops of CXCR1/2 (Allen et al., 2007), small-molecule antagonists appear to bind to allosteric sites at the 7-transmembrane domain, as demonstrated for repertaxin at CXCR1 (Bertini et al., 2004; Allegretti et al., 2005), or to a putative intracellular site of the CXCR2 receptor, as shown for the diarylurea SB332235 (Nicholls et al., 2008). Studies using radiolabeled SB265610 demonstrated competition between this member of the diarylurea class of antagonists and the structurally unrelated thiazolopyrimidine class (Walters et al., 2008), suggesting that both classes

share a common binding site (de Kruijf et al., 2009). Conversely, radiolabeled SB265610 failed to compete with structurally unrelated imidazolylpyrimidine antagonists (Ho et al., 2006; de Kruijf et al., 2009), supporting the notion that distinct allosteric antagonist sites exist on CXCR2 (Ho et al., 2006; de Kruijf et al., 2009). Although data are therefore available on the binding sites of some CXCR2 antagonists, more research is required to explore and define other target sites suitable for therapeutic development of CXCR2 antagonists.

Our CXCR2 inhibitor discovery program has focused on the nicotinamide glycolate pharmacophore. The data presented in this study support a mechanism of action for the carboxylic acid form of the pharmacophore at an intracellular site. Candidates for this site include (1) an allosteric intracellular site on CXCR2, as suggested for the diarylurea class of antagonists (Nicholls et al., 2008), (2) a site on an intracellular CXCR2-associated protein, and/or (3) a site formed as a result of a ternary complex between CXCR2 and another protein.

The nicotinamide glycolate ester exhibited no antagonist activity in cell-free assays, but the tritiated derivative was rapidly internalized by PMNs and de-esterified to the carboxylic acid in the cell interior, consistent with a model where the ester serves primarily as a lipophilic precursor that efficiently translocates into the intracellular space to liberate the active carboxylic acid. Indeed, the rates of de-esterification and passive diffusion (estimated by calculated logP values) in a series of related esters positively correlated with ester potency in antagonizing CXCL1-stimulated calcium flux in whole PMNs, supporting the pivotal role intracellular activation plays in the inhibitory mechanism of this class of compounds. Efflux of the active acid from PMNs was inhibited by probenecid, consistent the involvement of an organic acid transporter. Whereas up to 5 μM of the nicotinamide glycolate acid was inactive in whole-cell assays, the same compound inhibited calcium flux with an IC_{50} of 260 $\pm$ 30 nM after PMNs were

electroporated. Thus, direct evidence supporting the nicotinamide glycolate acid as the active intracellular antagonist was obtained using electroporation to directly load PMNs.

For studies involving radiolabeled nicotinamide glycolates, tritiated derivatives were prepared only for the nicotinamide glyclolates, where X = O (i.e. **3** and **4**), since the sulfur atom in derivatives **1** and **2** would have been incompatible with the palladium catalyst used in the tritiation reaction. Radiolabeled nicotinamide glycolate acid or ester did not bind to CXCR2 in Chinese hamster ovary (CHO) cell membranes at up to 5 μM (not shown). The reason for the absence of binding in membrane preparations is unclear. One possibility consistent with the observed inhibition of CXCL1-stimulated [^{35}S]GTPγS exchange by the nicotinamide glycolate acid is that a ternary complex of chemokine (CXCL1 or CXCL8) with CXCR2 may be required to place the receptor in a conformation permissive to nicotinamide glycolate binding. The absence of other required membrane-associated proteins in the artificial CHO cell membranes, or their loss during the membrane preparation process are alternative possibilities. Studies to explore these possibilities are underway.

Treatment of PMNs with the nicotinamide glycolate ester resulted in a dramatic intracellular accumulation of the active acid to levels 100- to 1000-fold greater than the extracellular ester concentration and in some cases reached millimolar concentrations. The concentrative accumulation of the acid indicated that the rate of ester uptake and intracellular de-esterification are together more rapid than the rate of efflux of the active carboxylic acid. Given the extent of accumulation, it is perhaps not surprising that CXCR2 inhibition, as measured by inhibition of calcium flux in PMNs, was sustained for at least 3.5 hours after washout of the ester from the extracellular space. For example, extrapolation of the loading and efflux kinetics of the tritiated ester derivative predicts an intracellular concentration of 60 μM for the active carboxylic

acid after 1.5 hours of washout, well above the sub- to low-micromolar potency observed for the carboxylic acid in cell-free assays and electroporated PMNs. Taken together, these data reconcile differences observed between the activity of the esters (methyl or benzyl) and the corresponding acid in electroporated PMNs. While the esters exhibited potent nanomolar (methyl ester) to subnanomolar (benzyl ester) activity in whole PMNs, the acid had weaker activity in electroporated PMNs. Due to the concentrative mechanism involved, the active acid was presumably able to attain the requisite intracellular concentration to antagonize CXCR2 from lower extracellular concentrations of the ester precursor.

As extensively reviewed by Beaumont *et al.*, ester prodrugs are most often used to enhance the lipophilicity, and thus the passive membrane permeability of water-soluble drugs through the intestinal barrier by masking charged groups such as carboxylic acids and phosphates (Beaumont et al., 2003). Once in the body, the ester bond is hydrolyzed to release the active principle into the circulation by ubiquitous esterases found in the intestine, blood, liver and other tissues, including carboxylesterases, acetylcholinesterases, butyrylcholinesterases, paraoxonases and arylesterases. The major aim of the prodrug approach is to quantitatively produce high concentrations of the active principle in the systemic circulation, not to mediate the entry of the prodrug into the target cell where the active principle would otherwise be unable to enter. The coupling of a cell-permeable but inactive ester precursor to intracellular liberation of the active antagonist in the target cell is thus an unusual delivery mechanism among ester prodrugs, with the lactone forms of HMG-CoA reductase inhibitors (e.g. lovastatin and simvastatin) that target hepatocytes and the CXCR2 antagonists that target PMNs reported herein being examples.

To our knowledge, the nicotinamide glycolate esters are the only reported CXCR2 antagonists that require intracellular activation, as reported here. The coupling of a cell-permeable but inactive ester precursor to intracellular liberation of the active antagonist is therefore unique among CXCR2 antagonists. This mechanism placed a challenging constraint on identifying ester congeners suitable for therapeutic implementation that required identifying a balance between the kinetics of intracellular activation and extracellular inactivation (i.e., in plasma), where both processes are mediated by de-esterification of the precursor. Cellular potency and instability in the plasma were thus invariably coupled to one another. The potential for rapid first-pass clearance by esterase activity in the intestine and liver were additional concerns. Ester forms that were highly potent *in vitro* necessarily exhibited rapid inactivation kinetics that precluded their usage *in vivo*. These features led us to abandon the nicotinamide glycolate ester pharmacophore from further development. However, the mechanism of ester activation elucidated herein gave us insight to strategies for developing new nicotinamide pharmacophore classes with therapeutic potential. One strategy we have pursued successfully is to identify new non-ester nicotinamide pharmacophore classes that are cell permeable and potent in the intracellular space but stable in the plasma. Our developments and *in vivo* results related to these new classes of nicotinamide antagonists will appear in subsequent reports.

Acknowledgements

We thank Laura Nelson (Department of Veterinary Molecular Biology, Montana State University, Bozeman, MT) for technical support.

References

Allegretti M, Bertini R, Cesta MC, Bizzarri C, Di Bitondo R, Di Cioccio V, Galliera E, Berdini V, Topai A, Zampella G, Russo V, Di Bello N, Nano G, Nicolini L, Locati M, Fantucci P, Florio S and Colotta F (2005) 2-Arylpropionic CXC chemokine receptor 1 (CXCR1) ligands as novel noncompetitive CXCL8 inhibitors. *J Med Chem* **48**:4312-4331.

Allen SJ, Crown SE and Handel TM (2007) Chemokine: receptor structure, interactions, and antagonism. *Annu Rev Immunol* **25**:787-820.

Auten RL, Richardson RM, White JR, Mason SN, Vozzelli MA and Whorton MH (2001) Nonpeptide CXCR2 antagonist prevents neutrophil accumulation in hyperoxia-exposed newborn rats. *J Pharmacol Exp Ther* **299**:90-95.

Banks C, Bateman A, Payne R, Johnson P and Sheron N (2003) Chemokine expression in IBD. Mucosal chemokine expression is unselectively increased in both ulcerative colitis and Crohn's disease. *J Pathol* **199**:28-35.

Beaumont K, Webster R, Gardner I and Dack K (2003) Design of ester prodrugs to enhance oral absorption of poorly permeable compounds: challenges to the discovery scientist. *Curr Drug Metab* **4**:461-485.

Beeh KM, Kornmann O, Buhl R, Culpitt SV, Giembycz MA and Barnes PJ (2003) Neutrophil chemotactic activity of sputum from patients with COPD: role of interleukin 8 and leukotriene B4. *Chest* **123**:1240-1247.

Bertini R, Allegretti M, Bizzarri C, Moriconi A, Locati M, Zampella G, Cervellera MN, Di Cioccio V, Cesta MC, Galliera E, Martinez FO, Di Bitondo R, Troiani G, Sabbatini V, D'Anniballe G, Anacardio R, Cutrin JC, Cavalieri B, Mainiero F, Strippoli R, Villa P, Di Girolamo M, Martin F, Gentile M, Santoni A, Corda D, Poli G, Mantovani A, Ghezzi P

and Colotta F (2004) Noncompetitive allosteric inhibitors of the inflammatory chemokine receptors CXCR1 and CXCR2: prevention of reperfusion injury. *Proc Natl Acad Sci U S A* **101**:11791-11796.

Bizzarri C, Beccari AR, Bertini R, Cavicchia MR, Giorgini S and Allegretti M (2006) ELR+ CXC chemokines and their receptors (CXC chemokine receptor 1 and CXC chemokine receptor 2) as new therapeutic targets. *Pharmacol Ther* **112**:139-149.

Bradley ME, Bond ME, Manini J, Brown Z and Charlton SJ (2009) SB265610 is an allosteric, inverse agonist at the human CXCR2 receptor. *Br J Pharmacol*:doi:10.1111/j.1476-5381.2009.00182.x.

Casilli F, Bianchini A, Gloaguen I, Biordi L, Alesse E, Festuccia C, Cavalieri B, Strippoli R, Cervellera MN, Di Bitondo R, Ferretti E, Mainiero F, Bizzarri C, Colotta F and Bertini R (2005) Inhibition of interleukin-8 (CXCL8/IL-8) responses by repertaxin, a new inhibitor of the chemokine receptors CXCR1 and CXCR2. *Biochem Pharmacol* **69**:385-394.

Cerretti DP, Kozlosky CJ, Vanden Bos T, Nelson N, Gearing DP and Beckmann MP (1993) Molecular characterization of receptors for human interleukin-8, GRO/melanoma growth-stimulatory activity and neutrophil activating peptide-2. *Mol Immunol* **30**:359-367.

Chapman RW, Phillips JE, Hipkin RW, Curran AK, Lundell D and Fine JS (2009) CXCR2 antagonists for the treatment of pulmonary disease. *Pharmacol Ther* **121**:55-68.

Cutshall NS, Kucera KA, Ursino R, Latham J and Ihle NC (2002) Nicotinanilides as inhibitors of neutrophil chemotaxis. *Bioorg Med Chem Lett* **12**:1517-1520.

de Kruijf P, van Heteren J, Lim HD, Conti PG, van der Lee MM, Bosch L, Ho KK, Auld D, Ohlmeyer M, Smit MJ, Wijkmans JC, Zaman GJ and Leurs R (2009) Nonpeptidergic

allosteric antagonists differentially bind to the CXCR2 chemokine receptor. *J Pharmacol Exp Ther* **329**:783-790.

DeLeo FR, Jutila MA and Quinn MT (1996) Characterization of peptide diffusion into electropermeabilized neutrophils. *J Immunol Methods* **198**:35-49.

Dwyer MP, Yu Y, Chao J, Aki C, Biju P, Girijavallabhan V, Rindgen D, Bond R, Mayer-Ezel R, Jakway J, Hipkin RW, Fossetta J, Gonsiorek W, Bian H, Fan X, Terminelli C, Fine J, Lundell D, Merritt JR, Rokosz LL, Kaiser B, Li G, Wang W, Stauffer T, Ozgur L, Baldwin J and Taveras AG (2006) Discovery of 2-hydroxy-N,N-dimethyl-3-{2-[[(R)-1-(5- methylfuran-2-yl)propyl]amino]-3,4-dioxocyclobut-1-enylamino}benzamide (SCH 527123): a potent, orally bioavailable CXCR2/CXCR1 receptor antagonist. *J Med Chem* **49**:7603-7606.

Erdem H, Pay S, Serdar M, Simsek I, Dinc A, Musabak U, Pekel A and Turan M (2005) Different ELR (+) angiogenic CXC chemokine profiles in synovial fluid of patients with Behcet's disease, familial Mediterranean fever, rheumatoid arthritis, and osteoarthritis. *Rheumatol Int* **26**:162-167.

Garau A, Bertini R, Mosca M, Bizzarri C, Anacardio R, Triulzi S, Allegretti M, Ghezzi P and Villa P (2006) Development of a systemically-active dual CXCR1/CXCR2 allosteric inhibitor and its efficacy in a model of transient cerebral ischemia in the rat. *Eur Cytokine Netw* **17**:35-41.

Geiser T, Dewald B, Ehrengruber MU, Clark-Lewis I and Baggiolini M (1993) The interleukin-8-related chemotactic cytokines GRO alpha, GRO beta, and GRO gamma activate human neutrophil and basophil leukocytes. *J Biol Chem* **268**:15419-15424.

Gonsiorek W, Fan X, Hesk D, Fossetta J, Qiu H, Jakway J, Billah M, Dwyer M, Chao J, Deno G, Taveras A, Lundell DJ and Hipkin RW (2007) Pharmacological characterization of Sch527123, a potent allosteric CXCR1/CXCR2 antagonist. *J Pharmacol Exp Ther* **322**:477-485.

Ho KK, Auld DS, Bohnstedt AC, Conti P, Dokter W, Erickson S, Feng D, Inglese J, Kingsbury C, Kultgen SG, Liu RQ, Masterson CM, Ohlmeyer M, Rong Y, Rooseboom M, Roughton A, Samama P, Smit MJ, Son E, van der Louw J, Vogel G, Webb M, Wijkmans J and You M (2006) Imidazolylpyrimidine based CXCR2 chemokine receptor antagonists. *Bioorg Med Chem Lett* **16**:2724-2728.

Holmes WE, Lee J, Kuang WJ, Rice GC and Wood WI (1991) Structure and functional expression of a human interleukin-8 receptor. *Science* **253**:1278-1280.

Keatings VM, Collins PD, Scott DM and Barnes PJ (1996) Differences in interleukin-8 and tumor necrosis factor-alpha in induced sputum from patients with chronic obstructive pulmonary disease or asthma. *Am J Respir Crit Care Med* **153**:530-534.

Koller DY, Nething I, Otto J, Urbanek R and Eichler I (1997) Cytokine concentrations in sputum from patients with cystic fibrosis and their relation to eosinophil activity. *Am J Respir Crit Care Med* **155**:1050-1054.

Kurdowska A, Noble JM, Grant IS, Robertson CR, Haslett C and Donnelly SC (2002) Anti-interleukin-8 autoantibodies in patients at risk for acute respiratory distress syndrome. *Crit Care Med* **30**:2335-2337.

Lally F, Smith E, Filer A, Stone MA, Shaw JS, Nash GB, Buckley CD and Rainger GE (2005) A novel mechanism of neutrophil recruitment in a coculture model of the rheumatoid synovium. *Arthritis Rheum* **52**:3460-3469.

Merritt JR, Rokosz LL, Nelson KH, Jr., Kaiser B, Wang W, Stauffer TM, Ozgur LE, Schilling A, Li G, Baldwin JJ, Taveras AG, Dwyer MP and Chao J (2006) Synthesis and structure-activity relationships of 3,4-diaminocyclobut-3-ene-1,2-dione CXCR2 antagonists. *Bioorg Med Chem Lett* **16**:4107-4110.

Moriconi A, Cesta MC, Cervellera MN, Aramini A, Coniglio S, Colagioia S, Beccari AR, Bizzarri C, Cavicchia MR, Locati M, Galliera E, Di Benedetto P, Vigilante P, Bertini R and Allegretti M (2007) Design of noncompetitive interleukin-8 inhibitors acting on CXCR1 and CXCR2. *J Med Chem* **50**:3984-4002.

Murphy PM and Tiffany HL (1991) Cloning of complementary DNA encoding a functional human interleukin-8 receptor. *Science* **253**:1280-1283.

Nibbering PH, Zomerdijk TP, Corsel-Van Tilburg AJ and Van Furth R (1990) Mean cell volume of human blood leucocytes and resident and activated murine macrophages. *J Immunol Methods* **129**:143-145.

Nicholls DJ, Tomkinson NP, Wiley KE, Brammall A, Bowers L, Grahames C, Gaw A, Meghani P, Shelton P, Wright TJ and Mallinder PR (2008) Identification of a putative intracellular allosteric antagonist binding-site in the CXC chemokine receptors 1 and 2. *Mol Pharmacol* **74**:1193-1202.

Podolin PL, Bolognese BJ, Foley JJ, Schmidt DB, Buckley PT, Widdowson KL, Jin Q, White JR, Lee JM, Goodman RB, Hagen TR, Kajikawa O, Marshall LA, Hay DW and Sarau HM (2002) A potent and selective nonpeptide antagonist of CXCR2 inhibits acute and chronic models of arthritis in the rabbit. *J Immunol* **169**:6435-6444.

Reich K, Garbe C, Blaschke V, Maurer C, Middel P, Westphal G, Lippert U and Neumann C (2001) Response of psoriasis to interleukin-10 is associated with suppression of

cutaneous type 1 inflammation, downregulation of the epidermal interleukin-8/CXCR2 pathway and normalization of keratinocyte maturation. *J Invest Dermatol* **116**:319-329.

Siemsen DW, Schepetkin IA, Kirpotina LN, Lei B and Quinn MT (2007) Neutrophil isolation from nonhuman species. *Methods Mol Biol* **412**:21-34.

Walters I, Austin C, Austin R, Bonnert R, Cage P, Christie M, Ebden M, Gardiner S, Grahames C, Hill S, Hunt F, Jewell R, Lewis S, Martin I, David N and David R (2008) Evaluation of a series of bicyclic CXCR2 antagonists. *Bioorg Med Chem Lett* **18**:798-803.

White JR, Lee JM, Young PR, Hertzberg RP, Jurewicz AJ, Chaikin MA, Widdowson K, Foley JJ, Martin LD, Griswold DE and Sarau HM (1998) Identification of a potent, selective non-peptide CXCR2 antagonist that inhibits interleukin-8-induced neutrophil migration. *J Biol Chem* **273**:10095-10098.

Footnotes

Financial Support

This work was supported by the National Institutes of Health National Heart Lung and Blood Institute [Grant R44HL072614] (D.Y.M.); and the National Institutes of Health National Center for Research Resources [Grant RR020185] (M.T.Q.).

Address correspondence to:

Dr. Dean Y. Maeda, Syntrix Biosystems, Inc., 215 Clay Street NW, Suite B-5, Auburn, WA 98001. E-mail: dmaeda@syntrixbio.com

Legends for Figures

Fig. 1. Selected members of the nicotinamide glycolate pharmacophore class.

Fig. 2. Schematic showing the synthesis of [^{3}H]-**3** and [^{3}H]-**4**. i) EEDQ, 4-fluoroaniline in DMF (72%); ii) NaH dispersion in mineral oil, methyl glycolate in THF (55%); iii) $^3H_2$ (g), 10% Pd/C in EtOH; iv) 1 N LiOH in MeOH (quant.). See Data Supplement for detailed experimental procedures and characterization data.

Fig. 3. Uptake of [^{3}H]-**3** (*upper*) and [^{3}H]-**4** (*lower*) in PMNs. Following incubation of PMNs with the indicated concentrations of [^{3}H]-**3** or [^{3}H]-**4**, aliquots were washed and centrifuged at the indicated times. The molar amount of radioactivity internalized was determined by measuring the radioactivity in the cell pellet by scintillation and correlating this to a calibration curve prepared separately with [^{3}H]-**3** and [^{3}H]-**4** (*not shown*). Data show the mean molar amount of internalized radioactivity from triplicate determinations.

Fig. 4. Representative chromatogram demonstrating separation of a comixture of the ester [^{3}H]-**3** from the acid [^{3}H]-**4** (panel A). Intracellular conversion of [^{3}H]-**3** to [^{3}H]-**4** (panel B). PMNs were incubated with 5 μCi of [^{3}H]-**3**, washed, lysed at the indicated times, and the lysates were subjected to reverse-phase HPLC and scintillation counting. Radioactivity in peaks with retention times corresponding to **3** and **4** were integrated to determine the relative amounts of intracellular [^{3}H]-**3** and [^{3}H]-**4**, respectively. Data show the mean intracellular radioactivity of each compound from triplicate determinations.

Fig. 5. De-esterification of nicotinamide glycolate esters by human plasma. Esters were incubated in human plasma at 37 ^{o}C at a concentration of 1 μM. Experiments were performed in replicate (n = 5), and aliquots were removed at the time points specified and analyzed by LC-MS/MS detection operating in multiple reaction monitoring (MRM) mode.

Fig. 6. Dose-dependent inhibition of CXCL1-stimulated calcium flux in electroporated PMNs treated with the nicotinamide glycolate acid **2**. Isolated PMNs were electroporated and treated with buffer (control) or **2** (at extracellular concentration of 100, 500 or 1000 nM) immediately after electroporation (**2** was dissolved in buffer without DMSO). After resealing, the cells were loaded with Fura-2 dye, and calcium flux was analyzed. Data show the mean CXCL1-stimulated calcium flux for each indicated extracellular concentration of **2** and the untreated control, each determined in triplicate. Significant differences relative to the untreated control are indicated (**$p < 0.01$, one-way ANOVA, Dunnett's multiple comparison test).

Fig. 7. Efflux of [^{3}H]-**4** from PMNs. PMNs ($6x10^{7}$ cells in 8 ml HBSS) were incubated with [^{3}H]-**3** (20 μCi, 2.7 μM) for 20 min, washed, and resuspended in 20 ml HBSS. At the indicated times, cells were centrifugated, and supernatants analyzed by reverse-phase HPLC and scintillation counting. Radioactivity was only detected in fractions with retention times corresponding to the retention time of [^{3}H]-**4**. No precursor [^{3}H]-**3** was detectable, confirming cell loading of only the carboxylic acid [^{3}H]-**4**. The mean amount (n = 3 – 4) of [^{3}H]-**4** in the supernatant was quantified at the indicated times by integrating peak radioactivity in each radiochromatogram. Significant differences relative to the 5 minute time are indicated (**$p < 0.01$, one-way ANOVA, Dunnett's multiple comparison test).

Fig. 8. Effect of probenecid on efflux of [^{3}H]-**4** from PMNs. PMNs ($6x10^7$ PMNs in 8 ml HBSS) were incubated with the precursor methyl ester [^{3}H]-**3** (20 μCi, 2.7 μM) for 20 min in order to load cells with the carboxylic acid [^{3}H]-**4**. The cells were then washed and resuspended in 25 ml HBSS, and incubated with and without 2 mM probenecid. At the indicated time points, cells were centrifugated and the radioactivity in the supernatant and pellet quantified by scintillation and expressed as a percentage of the initial intracellular radioactivity. Data show the mean percentage of radioactivity in the supernatant and cell pellet from triplicate determinations. Probenecid significantly affected the accumulation into the supernatant and loss from the cell pellet (***$p < 0.001$, two-way ANOVA).

Fig. 9. Inhibition of CXCL1-stimulated calcium flux in PMNs after methyl ester **1** washout. PMNs were incubated with either buffer (buffer-incubated PMNs) or 1 μM methyl ester **1** (ester-incubated PMNs) for 30 min, loaded with Fura-2 dye, washed and resuspended in assay buffer. Aliquots from buffer-incubated PMNs were removed at each indicated time, and intracellular calcium levels were measured after stimulation with (positive control fluorescence) or without (negative control fluorescence) 50 nM CXCL1. Aliquots from ester-incubated PMNs were removed at the same times, and intracellular calcium levels were measured after stimulation with 50 nM CXCL1 (response fluorescence). The mean % inhibition of methyl ester **1** on CXCL1-stimulated calcium flux was determined at the indicated times after ester washout, where % inhibition = 100 x (1 – ((response fluorescence – negative control fluorescence)/(positive control fluorescence – negative control fluorescence))). The data are presented as the mean $\pm$ S.E. from three independent experiments.

JPET Fast Forward. Published on September 24, 2009 as DOI: 10.1124/jpet.109.159020
This article has not been copyedited and formatted. The final version may differ from this version.

TABLE 1

Pharmacologic parameters of the nicotinamide glycolates **1** – **4**.

Compound	CXCL1 Chemotaxis[a,b] (IC_{50}, nM)	CXCL1 Ca^{2+} Flux[b] (IC_{50}, nM)	[^{125}I]-CXCL8 Binding[a,c] (IC_{50}, nM)	CXCL1 [^{35}S]GTPγS[a,c] (IC_{50}, nM)
1	42	48	>10000[d]	>5000
2	>20000	>5000	1200	614
3	110	68	>10000	N.D.
4	>20000	>5000	N.D.	N.D.

N.D. = not determined. Values are the geometric mean of two or more determinations.

[a]Values as reported in Cutshall *et al* (Cutshall et al., 2002).

[b]PMNs.

[c]Membrane preparations from CHO cells stably expressing CXCR2.

[d]Same for [^{125}I]-CXCL1 binding (MDS Pharma Services, Bothell, WA).

JPET Fast Forward. Published on September 24, 2009 as DOI: 10.1124/jpet.109.159020
This article has not been copyedited and formatted. The final version may differ from this version.

TABLE 2

Antagonism of CXCL-1 stimulated calcium flux in PMNs and de-esterification by esterase activity in human plasma.

Compound	Ester R Group	CXCL1 Ca^{2+} Flux (IC_{50}, nM)	Plasma Half-Life[a] (min)	LogP[b]
1	methyl	48	60	2.6
5	benzyl	0.2	60	4.2
6	*t*-butyl	>10000	>240	3.7

[a]Esterase activity in human plasma at 37 ^{o}C using a compound concentration of 1 μM.

[b]Octanol:water partition coefficient calculated using the Molinspiration property engine v2009.01 according to the miLogP2.2 method (http://www.molinspiration.com).

Figure 1

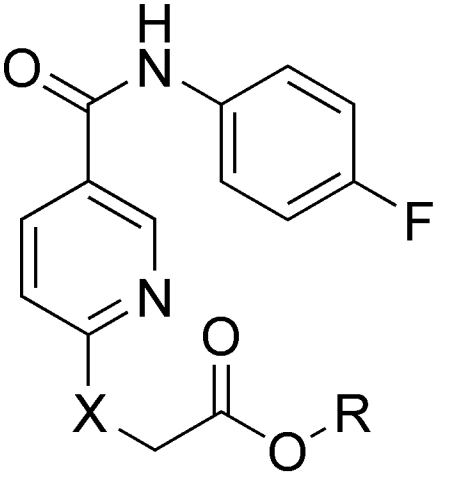

1: X = S, R = methyl
2: X = S, R = H
3: X = O, R = methyl
4: X = O, R = H
5: X = S, R = benzyl
6: X = S, R = *t*-butyl

Figure 2

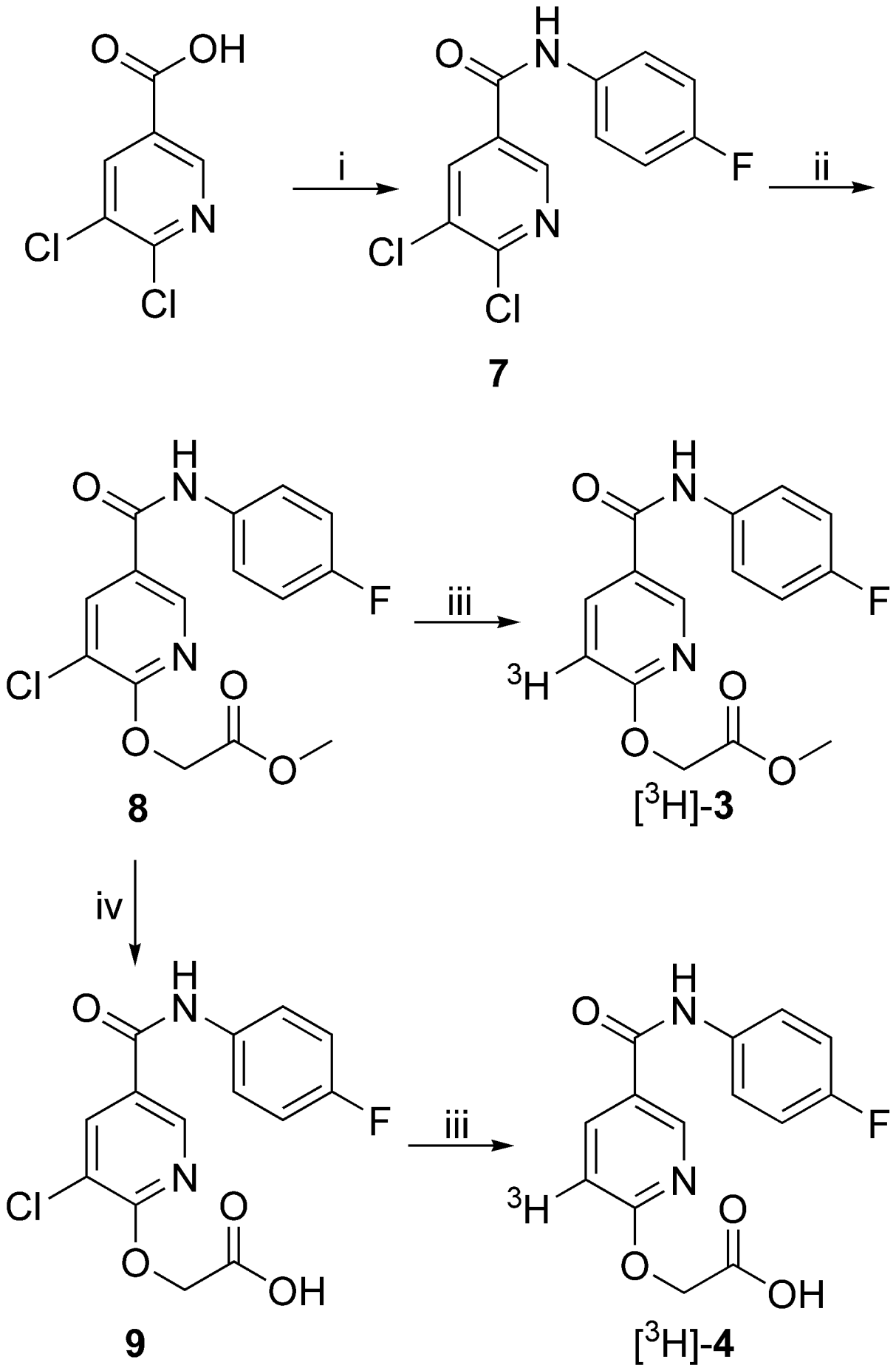

Figure 3

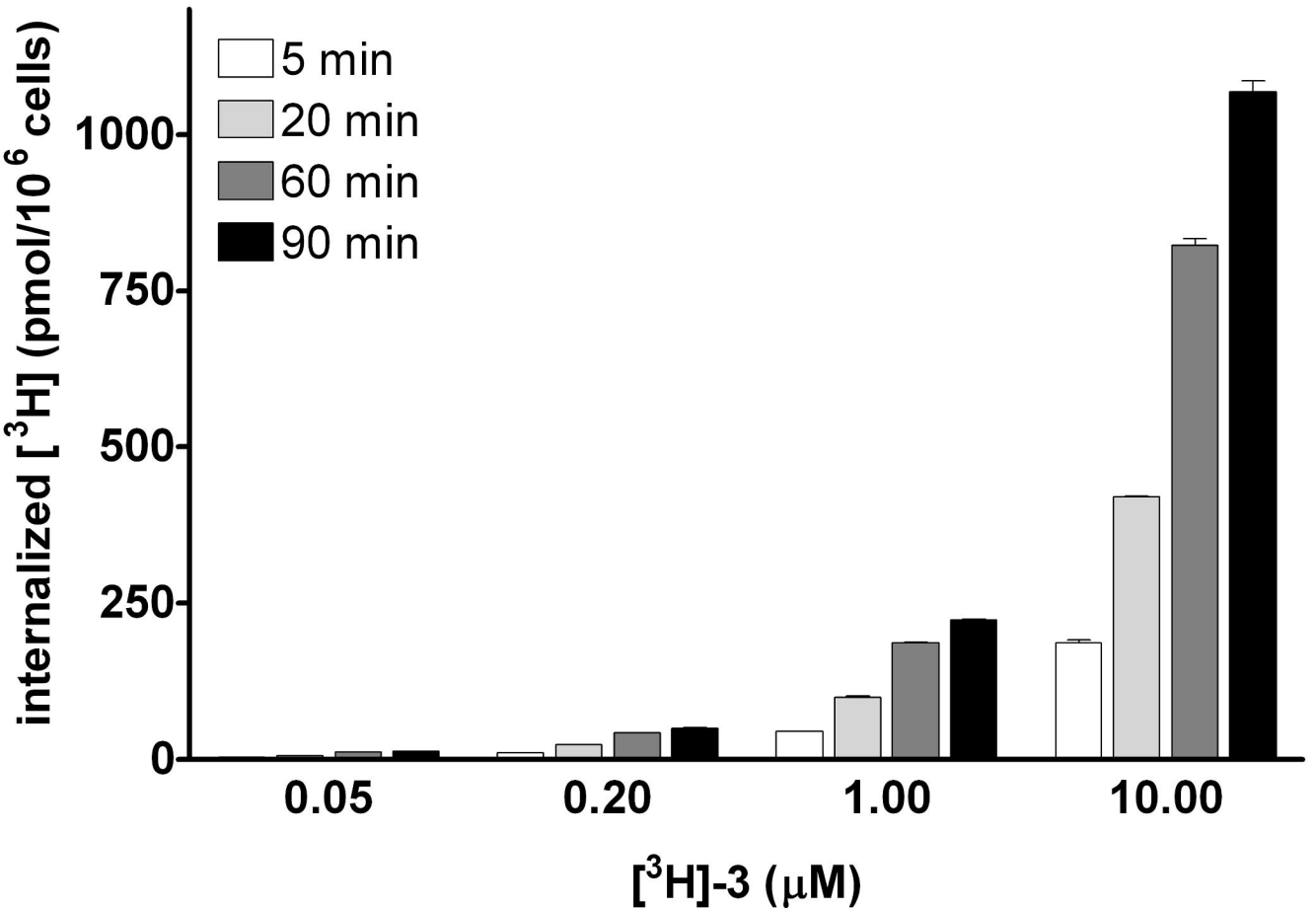
5 min
20 min
60 min
90 min
internalized [3H] (pmol/10^6 cells)
1000
750
500
250
0
0.05
0.20
1.00
10.00
[3H]-3 (μM)

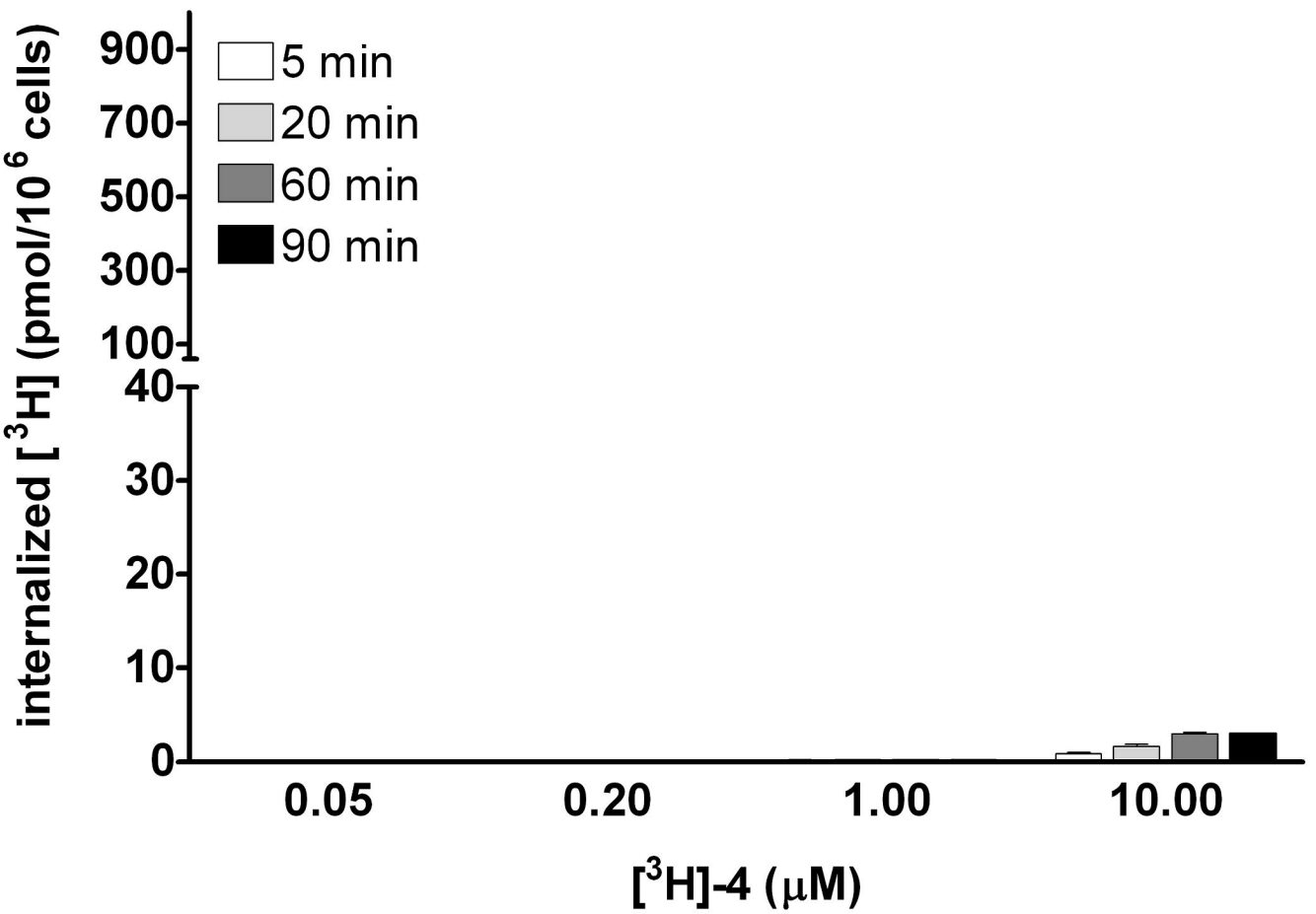
5 min
20 min
60 min
90 min
internalized [3H] (pmol/10^6 cells)
900
700
500
300
100
40
30
20
10
0
0.05
0.20
1.00
10.00
[3H]-4 (μM)

Figure 4

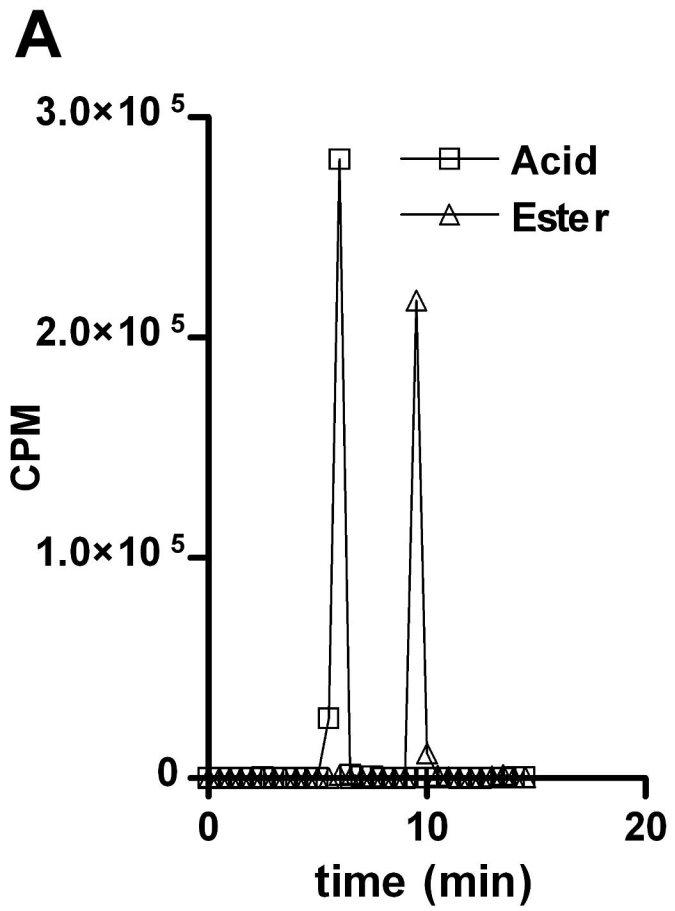
A
3.0×10 5
2.0×10 5
1.0×10 5
0
CPM
Acid
Ester
0
10
20
time (min)

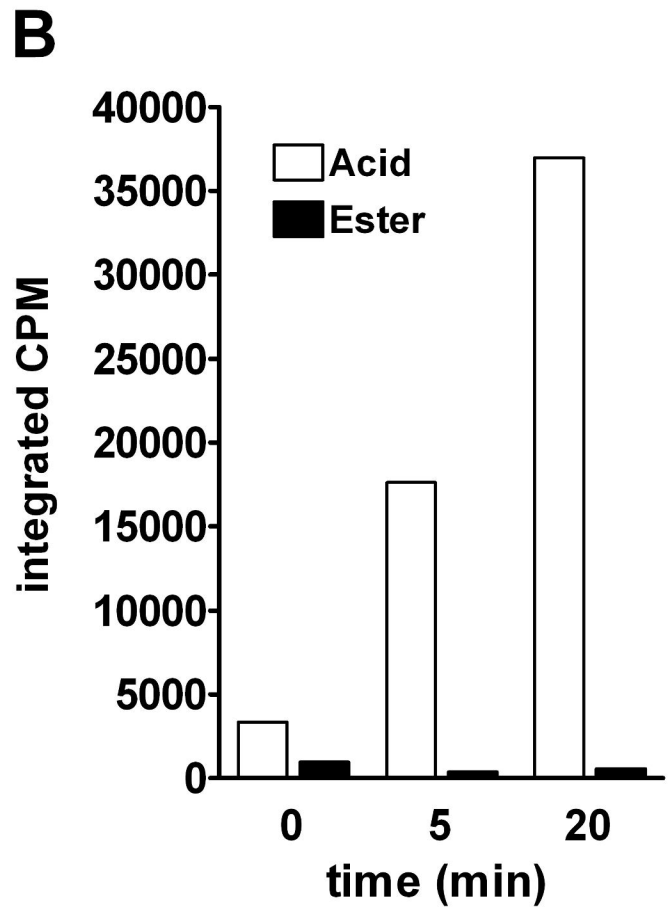
B
40000
35000
30000
25000
20000
15000
10000
5000
0
integrated CPM
Acid
Ester
0
5
20
time (min)

Figure 5

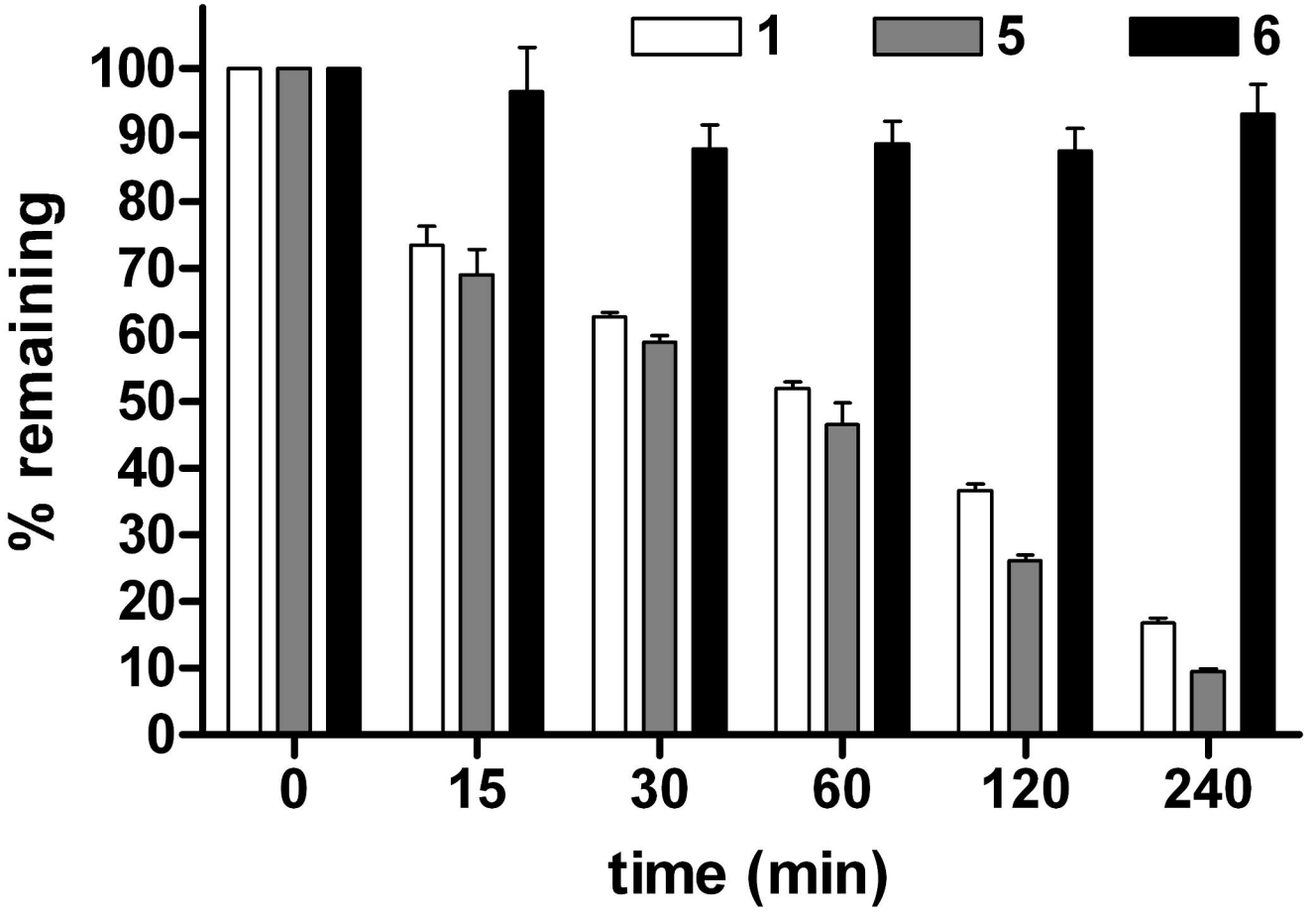
1
5
6
100
90
80
70
60
50
40
30
20
10
0
% remaining
0
15
30
60
120
240
time (min)

Figure 6

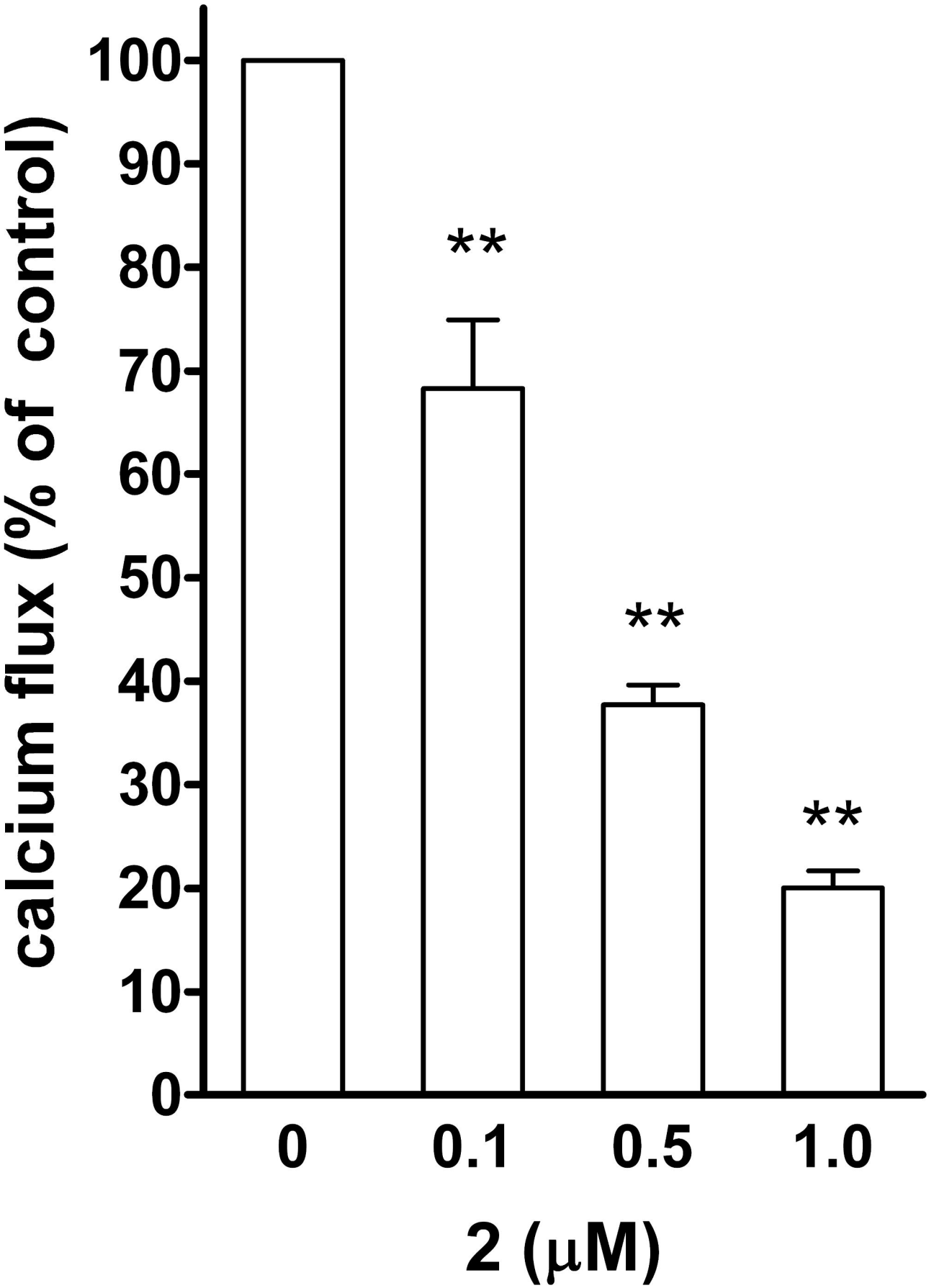
calcium flux (% of control)
100
90
80
70
60
50
40
30
20
10
0
**
**
**
0
0.1
0.5
1.0
2 (μM)

Figure 7

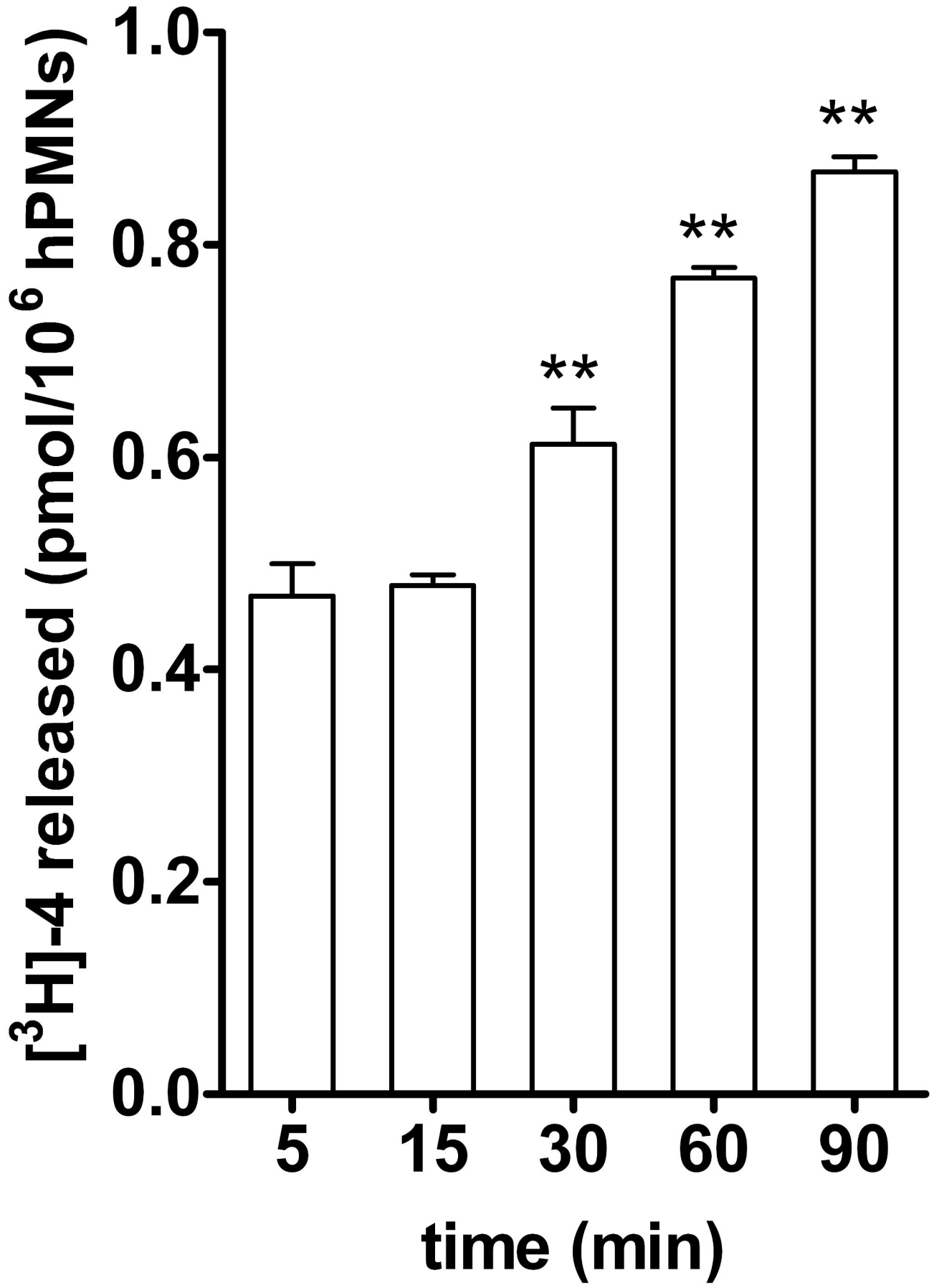
[3H]-4 released (pmol/10^6 hPMNs)
1.0
0.8
0.6
0.4
0.2
0.0
**
**
**
5
15
30
60
90
time (min)

Figure 8

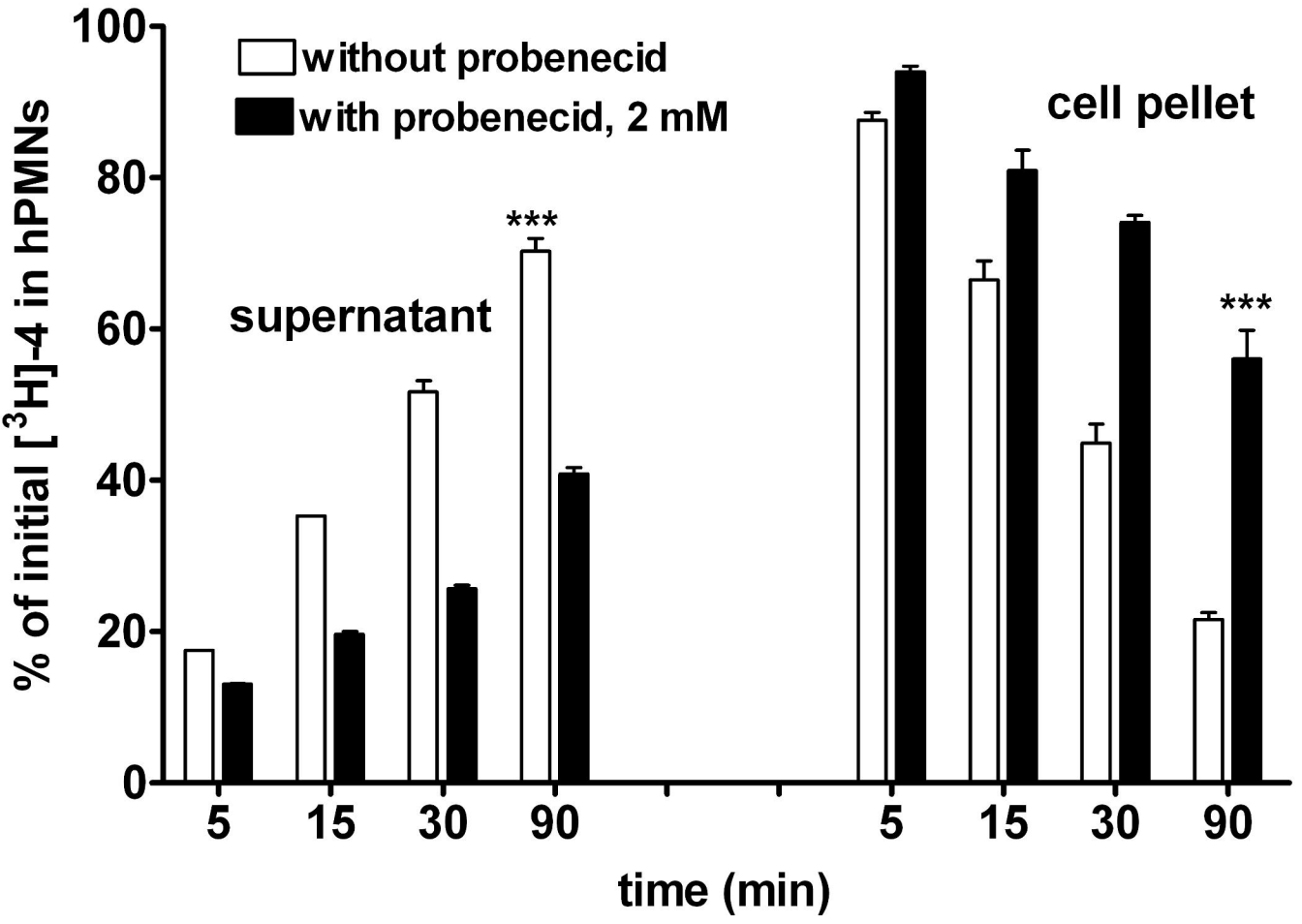
without probenecid
with probenecid, 2 mM
supernatant
cell pellet
***
***
% of initial [3H]-4 in hPMNs
100
80
60
40
20
0
5
15
30
90
5
15
30
90
time (min)

Figure 9

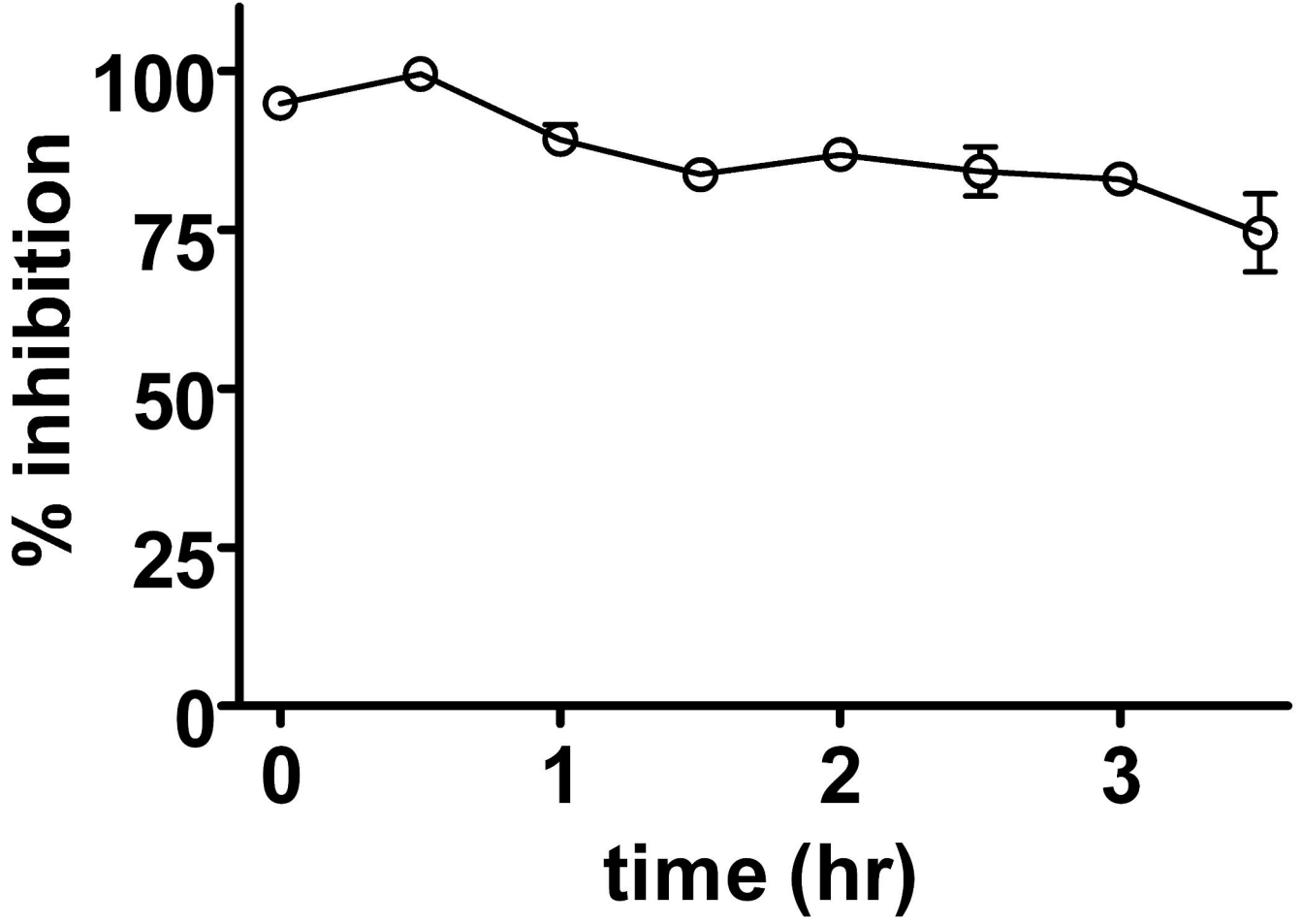

General Synthesis and Characterization Methods

Synthetic reaction progression was monitored by TLC using precoated aluminum backed silica gel plates with fluorescent indicator (EMD Chemicals, Gibbstown, NJ). ^{1}H NMR (300.1 MHz) spectra were recorded on a Bruker AV300 spectrometer. MS spectra were recorded on a Micromass Quattro II mass spectrometer (Waters, Milford, MA), operating under positive ion mode using an electrospray ionization probe, connected to a Shimadzu 10AD HPLC system (Shimadzu, Kyoto, Japan) equipped with a UV detector (SPD-10AVvp), two pumps (LC-10ADvp), an autosampler (SIL-HT), degasser (DGU-14A) and a column oven (CTO-10AC). Reverse-phase HPLC separations were performed with a Phenomenex Gemini C_{18} column (2.0 x 50 mm; 110 Å, 5 μm) at 35 °C utilizing gradient elution (5 – 95% B over 12 min, solvent A = 0.1% formic acid/H_2O, solvent B = 0.1% formic acid/MeCN, flow rate = 0.2 ml/min, l = 254 nm). The purity of all compounds was determined to be ≥ 95% by reverse-phase HPLC.

Synthesis of [5-(4-fluoro-phenylcarbamoyl)-pyridin-2-ylsulfanyl]-acetic acid benzyl ester 5

To a solution of *N*-(4-fluoro-phenyl)-6-mercapto-nicotinamide [0.25 g, 1 mmol, 1 eq. (as prepared by Cutshall *et al.* 2002)] in anhydrous dimethylformamide (2 ml), benzyl bromoacetate (0.16 ml, 1 mmol, 1 eq.) was added, followed by triethylamine (0.14 ml, 1 mmol, 1 eq.). A crystalline material immediately formed. After 1 hour at room temperature, the reaction mixture was diluted into ethyl acetate (50 ml) and the organic layer washed with water, 0.1 N aq. HCl, water, brine, and dried over Na_2SO_4. The reaction was filtered, and the solvent removed by rotary evaporation. The crude material was purified by silica gel column chromatography (ethyl acetate/hexanes, 1:2 as eluent) to yield 278 mg (70%) as an off white solid. TLC R_f (ethyl acetate/hexanes, 1:1) = 0.60; HPLC R_t = 11.21 min; $[MH]^+$ (ESI-MS) = 397.01; ^{1}H NMR (300

MHz, d_6-DMSO) δ 4.19 (s, 9H), 5.16 (s, 2H), 7.21 (t, 2H), 7.34 (m, 5H), 7.53 (d, 1H), 7.78 (dd, 2H), 8.14 (dd, 1H), 8.88 (dd, 1H), 10.34 (s, 1H).

Synthesis of [5-(4-fluoro-phenylcarbamoyl)-pyridin-2-ylsulfanyl] acetic acid *tert*-butyl ester 6

To a solution of *N*-(4-fluoro-phenyl)-6-mercapto-nicotinamide [0.25 g, 1 mmol, 1 eq. (as prepared by Cutshall *et al.* 2002)] in anhydrous dimethylformamide (2 ml), *tert*-butyl bromoacetate (0.15 ml, 1 mmol, 1 eq.) was added, followed by triethylamine (0.14 ml, 1 mmol, 1 eq.). A crystalline material immediately formed. After 1 hour at room temperature, the reaction mixture was diluted into ethyl acetate (50 ml) and the organic layer washed with water, 10% aq. citric acid, water, brine, and dried over Na_2SO_4. The reaction was filtered, and the solvent removed by rotary evaporation. The crude material was purified by silica gel column chromatography (ethyl acetate/hexanes, 1:2 as eluent) to yield 199 mg (55%) as an off white solid. TLC R_f (ethyl acetate/hexanes, 1:1) = 0.77; HPLC R_t = 11.46 min; $[MH]^+$ (ESI-MS) = 307.06; ^{1}H NMR (300 MHz, d_6-DMSO) d 1.41 (s, 9H), 4.00 (s, 2H), 7.21 (t, 2H), 7.51 (d, 1H), 7.76 (dd, 2H), 8.15 (dd, 1H), 8.93 (s, 1H).

Synthesis of 5,6-dichloro-*N*-(4-fluoro-phenyl)-nicotinamide 7

To a solution of 5,6-dichloronicotinic acid (3.84 g, 20 mmol, 1 eq.) and 4-fluoroaniline (2.22 g, 20 mmol, 1 eq.) in dimethylformamide (60 ml) was added 2-ethoxy-1-ethoxycarbonyl-1,2-dihydroquinoline (EEDQ, 4.94 g, 20 mmol, 1 eq.). The reaction solution was stirred at room temperature under nitrogen overnight. The reaction solution was then diluted into ethyl ether (100 ml) and washed with water, 0.1 N aq. HCl, water, 5% aq. $NaHCO_3$, water, brine, and dried over $MgSO_4$. The mixture was filtered, and the solvent was removed by rotary evaporation to

yield 4.087 g (72%) as an off white solid. TLC R_f (ethyl acetate/hexanes, 1:2) = 0.38; HPLC R_t = 10.78 min; $[MH]^+$ (ESI-MS) = 286.81; ^1H NMR (300 MHz, d_6-DMSO) δ 7.24 (t, 2H), 7.76 (dd, 2H), 8.62 (d, 1H), 8.89 (d, 1H), 10.60 (s, 1H).

Synthesis of [3-chloro-5-(4-fluoro-phenylcarbamoyl)-pyridin-2-ylsulfanyl]-acetic acid methyl ester 8

To a solution of 5,6-dichloronicotinamide **7** (1.2 g, 4.2 mmol, 1 eq.) and methyl glycolate (0.65 ml, 8.4 mmol, 2 eq.) in anhydrous tetrahydrofuran (40 ml) was added sodium hydride (60% dispersion in mineral oil, 0.34 g, 8.4 mmol, 2 eq.) under argon at room temperature. Vigorous bubbling was seen, and the reaction mixture became a cloudy yellow color. After 3 hours, the reaction mixture was diluted into ethyl acetate (100 ml), and the combined organic layer was washed with water, 0.1 N aq. HCl, water, brine, and dried over Na_2SO_4. The mixture was filtered, and the solvent was removed by rotary evaporation to yield an oil. The oil was purified by silica gel column chromatography (ethyl acetate/hexanes, 1:3 as eluent) to yield 0.78 g (55%) as a white solid. TLC R_f (ethyl acetate/hexanes 1:2) = 0.43; HPLC R_t = 10.63 min; [MH]+ (ESI-MS) = 339.01; ^1H NMR (300 MHz, d_6-DMSO) δ 3.70 (s, 3H), 5.12 (s, 2H), 7.21 (t, 2H), 7.75 (dd, 2H), 8.44 (d, 1H), 8.64 (d, 1H), 10.38 (1H).

Synthesis of [3-chloro-5-(4-fluoro-phenylcarbamoyl)-pyridin-2-ylsulfanyl]-acetic acid 9

To a solution of methyl ester **8** (0.2 g, 0.64 mmol, 1 eq.) in methanol (15 ml) was added 1 N aq. LiOH (1.3 ml, 1.3 mmol, 2 eq.) at room temperature. After 2 hours, the reaction mixture was concentrated by rotary evaporator and diluted into 0.1 N HCl (15 ml) and cooled at 5 ^oC overnight. The resulting precipitate was filtered, washed with water and dried to yield 185 mg (100%) as a white solid. TLC R_f (1% acetic acid/ethyl acetate) = 0.26; HPLC R_t = 9.83 min;

$[MH]^+$ (ESI-MS) = 325.10; ^{1}H NMR (300 MHz, d_4-MeOH) δ 5.03 (s, 2H), 7.09 (t, 2H), 7.67 (dd, 2H), 8.32 (d, 1H), 8.61 (d, 1H).

Synthesis of [^{3}H]-3 and [^{3}H]-4

The tritiation of **8** and **9** to afford [^{3}H]-**3** and [^{3}H]-**4**, respectively, and subsequent purification were performed at Moravek Biochemicals (Brea, CA, USA). The tritiated products were purified by C_{18} reverse phase preparative HPLC on a Thermo Finnigan P4000 system using 50% aq. EtOH with 0.1% TFA, l = 274 nm. The final purified [^{3}H]-**3** and [^{3}H]-**4** had radiochemical purities >99.7% with specific activities of 18 Ci/mmol.